JMEPEG (2012) 21:1283–1291
DOI: 10.1007/s11665-011-0030-1

1059-9495/$19.00

Electrochemical Behavior of 2205 Duplex Stainless Steel in NaCl Solution with Different Chromate Contents

H. Luo, C.F. Dong, X.Q. Cheng, K. Xiao, and X.G. Li

(Submitted December 14, 2010; in revised form July 25, 2011)

The electrochemical behavior of 2205 duplex stainless steel in NaCl solution with different chromate contents were investigated by potentiodynamic polarization curves, electrochemical impedance spectroscopy (EIS), Mott-Schottky analysis, and scanning electron microscope (SEM). The effect of chromate on passivity and pitting behavior of stainless steel was also studied. The results showed that pitting susceptibility as well as semiconducting properties of passive film is heavily dependent on the chromate concentration. There exists a critical chromate value (about 0.03 M in 1 M NaCl solutions) below which the pitting corrosion on the stainless steel would be inhibited and above which it would be accelerated.

Keywords chromate, corrosion, duplex stainless steel, NaCl

1. Introduction

Duplex stainless steels (DSS) have been increasingly used for a variety of application in marine construction, chemical industries and power plants, due to their excellent combination of mechanical properties and corrosion resistance (Ref 1). It is well known that such good properties of DSS strongly rely on a balanced two-phase microstructure consisting of approximately equal amount of austenite and ferrite (Ref 2).

Passivity is an important factor in determining the ability of stainless steel to resist corrosion. Investigation of the electrochemistry of a passivated metal can reveal not only the structure and composition, but also the electrochemical corrosion behavior of the film (Ref 2, 3). The passive film formed spontaneously on stainless steel surface has been widely studied by analysis techniques (Ref 3, 4). Pitting corrosion is a major cause of the stainless steel failure in various industrial applications. It is well known that under the action of aggressive ions, i.e., chloride anion, local breakdown of passivity occurs, mainly at sites of local heterogeneities, causing pitting corrosion (Ref 5). The growth of corrosion pits of stainless steel has been divided into three consecutive steps: initiation, metastable propagation, and stable propagation of pits (Ref 4).

Chromate used to be an efficient oxidant for metal and alloy passivation, but its use has been banned due to its toxicity. It can passivate metal by forming monatomic or polyatomic oxide film on the metal surface (Ref 6, 7). The chromates are very good inhibitors of pitting corrosion in stainless steels (Ref 7). A previous work (Ref 6-10) reported the effect of chromate on electrochemical and corrosion behavior of stainless steel. However, the pitting behavior of 2205 DSS in high concentration NaCl solution with addition of chromate has not been fully discussed.

In this study, the electrochemical behavior of 2205 DSS in 1 M NaCl solution with the presence of chromate was studied by electrochemical measurements in terms of potentiodynamic polarization, electrochemical impedance spectroscopy (EIS), and Mott-Schottky (M-S) technique. The role of this study is to establish a relationship between the chromate presence and pitting susceptibility. It is expected that the research would provide insight into the corrosion mechanism, in particular, the passivity and pitting of 2205 DSS in NaCl solution with different contents of chromate.

2. Experimental

2.1 Electrode and Solutions

All the specimens used in this study were fabricated from a sheet of 2205 DSS with the thickness of 5 mm. The chemical composition (wt.%) is shown in Table 1. The test specimens were embedded in epoxy resin with an exposed working area of 1 cm^2 for electrochemical measurements. The working surface was polished mechanically using successive grade emery papers up to 2000 grit. Then, the surface was polished with 0.1 μm alumina polishing powder, degreased with alcohol, cleaned in water, and finally dried in air.

The test solutions were 1 M NaCl solution with addition of 0.001, 0.005, 0.01, 0.03, 0.05, 0.1, 0.3, and 0.5 M Na_2CrO_4. All solutions were prepared from analytical grade and chemically pure reagents.

2.2 Electrochemical Measurements

Electrochemical measurements were performed using a PAR 2273 electrochemical system on a conventional three-electrode cell. The specimen was used as working electrode (WE), a platinum plate was used as counter electrode (CE) and a saturated calomel electrode (SCE) equipped with Luggin capillary was used as reference electrode (RE). All the

H. Luo, C.F. Dong, X.Q. Cheng, K. Xiao, and **X.G. Li**, Corrosion and Protection Center, University of Science and Technology Beijing, Beijing 100083, China. Contact e-mails: lixiaogang99@263.net and hongluo81@126.com.

Table 1 Chemical composition of 2205 duplex stainless steel (wt.%)

C	P	S	Cr	Ni	N	Mo	Mn	Si	Fe
0.014	0.023	0.001	22.39	5.68	0.17	3.13	1.38	0.39	Balance

potentials reported in this study were referred to the SCE. Before each measurement, the solution was purged with pure nitrogen for 1 h. In order to guarantee the reproducibility of the data, the electrochemical measurements were repeated at least three times. All the electrochemical tests were conducted at room temperature.

2.2.1 Potentiodynamic Polarization Curves. Prior to the measurement, the specimens were cathodically polarized at −0.8 V for 15 min to remove the pre-existing oxide film. The potentiodynamic polarization tests were conducted at a scanning rate of 1.5 mV/s from −0.8 V to a very anodic potential. Various electrochemical parameters were obtained from the polarization curves, i.e., corrosion potential (E_{corr}), corrosion current density (I_{corr}), passive current density (i_p), and pitting potential (E_p), the potential at which the current density exceeded 100 μA/cm^2 is defined as pitting potential.

2.2.2 EIS Measurements. The EIS was measured at open circuit potential (OCP) with a sinusoidal excitation potential of 10 mV in the frequency range from 100 kHz to 10 mHz. The measured EIS data was fitted by using Zview 2.70 software.

2.2.3 Mott-Schottky Analysis. M-S curves were obtained by measuring the capacitance of the passive film at a rate of 15 mV/step. The potential was scanned in the potential range from −600 to 1100 mV. An AC voltage of 10 mV (peak-to-peak) in frequency of 1000 Hz was applied to the system.

M-S plots are based on the M-S relation, which describes the potential dependence of the space charge capacity, C, of a semiconductor electrode under depletion condition (Ref 11)

$$\frac{1}{C^2} = \pm\frac{2}{eN\varepsilon\varepsilon_0}\left(|\Delta E| - \frac{kT}{e}\right), \quad \text{(Eq 1)}$$

where negative sign is for p-type and positive sign for n-type conductivity, e is the electron charge, N is the donor density for n-type semiconductor or the acceptor density for p-type semiconductor, ε is the relative dielectric constant of the semiconductor, ε_0 is the vacuum permittivity, 8.85×10^{-12} F/m, k is the Boltzmann's constant, and T is the absolute temperature. $|\Delta E| = |E - E_{fb}|$, E is the electrode potential and E_{fb} is the flat band potential. The donor or acceptor concentration and flat band potential can be determined from the experimental $C^{-2} \sim E$ plot. The type of the semiconductor also can be determined by the sign of the slope of $C^{-2} \sim E$ plot.

3. Results

3.1 Microstructure Characterization

Prior to the microstructure observation, the specimen was etched in aqua regia ($V_{\text{Nitric acid}}$:$V_{\text{Hydrochloric acid}}$ = 1:3) solution. Figure 1 shows the metallographic structure of 2205 DSS, which contains austenite and ferrite phases. The white region in Fig. 1 corresponds to austenitic phase, while the gray region is ferritic phase. And the island-like austenite is embedded in the continuous ferritic matrix.

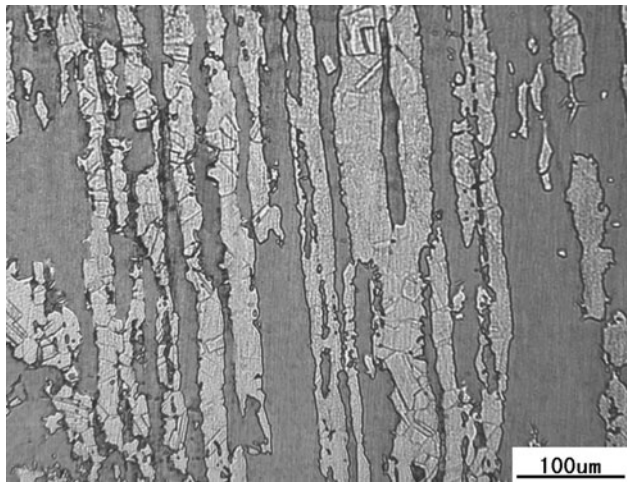

Fig. 1 Metallographic structures of 2205 duplex stainless steel

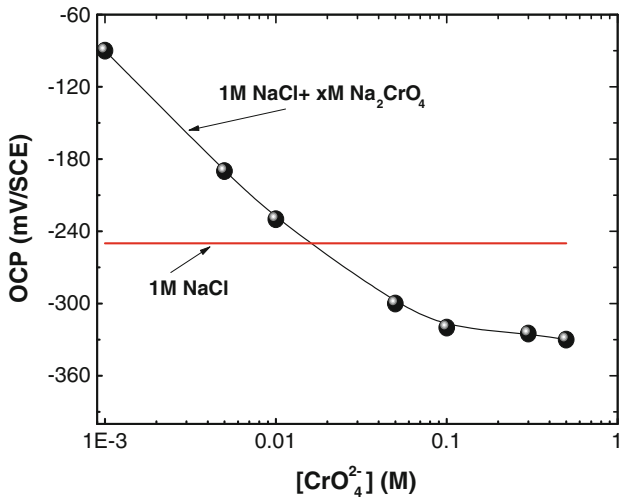

Fig. 2 Open circuit potential of 2205 duplex stainless steel in NaCl solutions with different Na_2CrO_4 concentrations

3.2 Open Circuit Potential Measurements

Figure 2 shows the OCP of 2205 DSS in 1 M NaCl solution with different contents of chromate. It is seen that OCP shifted gradually to negative direction with the increasing of chromate concentration. The OCP value in the absence of chromate is −250 mV. The OCP values measured in NaCl solution with chromate (<0.03 M) is positive than that measured in the absence of chromate. While the OCP measured in NaCl solution with chromate (>0.03 M) is negative than that measured in the absence of chromate. Thermodynamically, the more negative the OCP, the higher tendency the corrosion takes place.

3.3 Potentiodynamic Polarization Curve Measurements

Figure 3 shows the anodic part of polarization curves of 2205 DSS in 1 M NaCl solutions with and without chromate. There is an anodic oxidation peak at ~0.75 V, which probably attributes to the formation of Cr_2O_3 (Ref 10, 12) on the electrode surface:

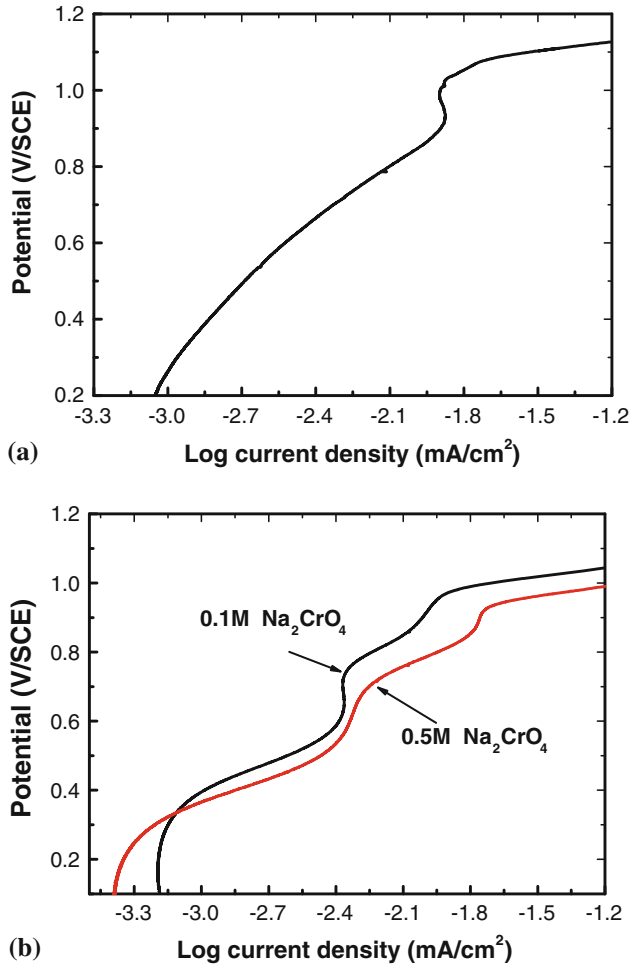

Fig. 3 Potentiodynamic polarization curves of 2205 duplex stainless steel: (a) in 1 M NaCl solution and (b) in NaCl solutions with 0.1 and 0.5 M Na_2CrO_4

$$2CrO_4^{2-} + 10H^+ + 6e \rightarrow Cr_2O_3 + 5H_2O \quad \text{(Eq 2)}$$

Similar results were obtained by Igual Muñoz et al. (Ref 10) and Carmezim et al. (Ref 13).

The potentiodynamic polarization curves of the 2205 DSS in 1 M NaCl solutions containing 0, 0.001, 0.01, 0.1, and 0.5 M chromate are shown in Fig. 4. It is found that polarization curves have the similar trends with different concentration of chromate. They are characterized by an extreme low anodic current density and wide range of passive regions (−450 to 1100 mV).

Figure 5 shows the passive current density of 2205 DSS in NaCl solution with different concentrations of chromate. The i_p measured in NaCl solution without chromate is 0.8 μA/cm^2, which is much higher than that with addition of chromate. There is a critical chromate concentration of 0.03 M, where the i_p is the smallest. Chromate can passivate steel surface by forming insoluble films as well as promote corrosion by activating cathodic reaction (Ref 10, 12, 14). As shown in Fig. 5, when the chromate concentration is 0.03 M (from 0.001 to 0.5 M), the passive current density reaches minimum value. Combined with the OCP values shown in the Fig. 2, the chromate in high concentration is corrosion accelerator and in low concentration as corrosion inhibitor.

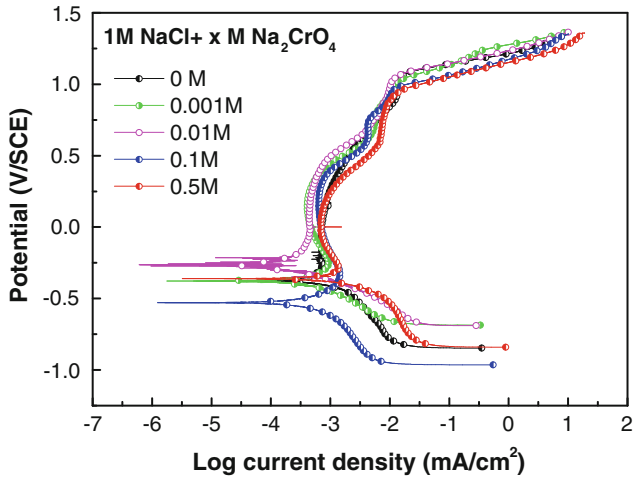

Fig. 4 Potentiodynamic polarization curves of 2205 duplex stainless steel in 1 M NaCl solutions with 0, 0.001, 0.01, 0.1, and 0.5 M Na_2CrO_4

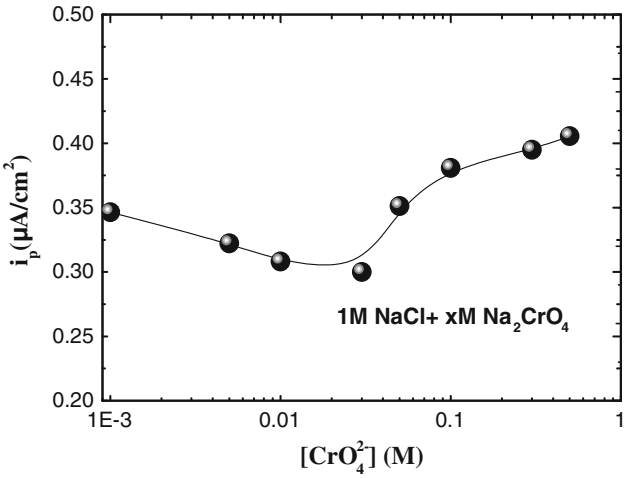

Fig. 5 Variation of the passive current densities of 2205 duplex stainless steel as a function of CrO_4^{2-} anion concentration

Figure 6 shows the relationship between chromate concentration and pitting potential. It is seen that pitting potential increased with decreasing of chromate concentration. The pitting potential in the absence of chromate is 1.12 V. Therefore, the pitting potential in solution with chromate (<0.03 M) is positive than that measured in the absence of chromate. While the pitting potential in solution with chromate (>0.03 M) is negative than that in the absence of chromate. This result further confirms that chromate acts as a corrosion inhibitor for 2205 DSS at low chromate concentration, and acts as corrosion accelerator at high concentration.

3.4 SEM Observations

Figure 7 shows the surface morphologies of the samples after electrochemical tests. Some pits are observed on the surface. As shown in Fig. 7(a)-(e), the number and diameter of the pit decreased when the chromate concentration increased from 0 to 0.03 M, and then increased as the chromate concentration increased from 0.03 to 0.5 M. With consideration of the passive current density, the most stable passive film was

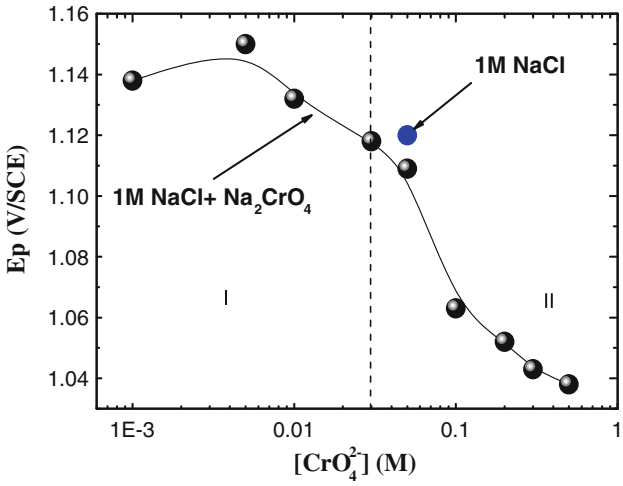

Fig. 6 Variation of the pitting potential of 2205 duplex stainless steel as a function of CrO_4^{2-} anion concentration

obtained in NaCl solution with 0.03 M chromate. Therefore, the corrosion behavior, i.e., passive film formation, pitting corrosion, of 2205 DSS is heavily dependent on the chromate concentration.

3.5 Mott-Schottky Analysis

Figure 8 shows the M-S plots of the passive film formed on 2205 DSS surface in 1 M NaCl solution without chromate. In zone (I), the positive slope indicates that the passive film is n-type semiconductor, in zone (II), the negative slope indicates that the passive film is p-type semiconductor (Ref 14).

The M-S plots of the passive film formed on the sample surface in 1 M NaCl solution containing different concentrations of chromate are shown in Fig. 9. All the M-S plots are characterized by three zones: zone (I) and (III) with same characteristics are n-type semiconductor, while zone (II) is p-type semiconductor. The existence of negative and positive slopes in the curves has been interpreted as the representative of a capacitance behavior. With an inner p-type semiconducting region formed by chromium oxide and an outer n-type semiconducting region formed by iron oxide (Ref 15, 16). At the potential between 0.3 and 0.85 V, the type of semiconductor changes from p-type to n-type, indicating the main components of passive film change from chromium oxide to iron oxide with potential.

According to Eq 1, the acceptor (N_A) or donor densities (N_D) can be calculated by using the slopes of the straight lines in different regions. The calculated results are summarized in Table 2. According to results of Table 2, the passive film presents a high density of doping species, doping species are structural defects, such as cations, anion vacancies, and interstitial cations (Ref 15). The acceptor and donor densities of the passive film formed in NaCl solution without chromate are higher than that containing chromate. The passive film formed in NaCl solution without chromate exhibits extremely high donor densities ($1\text{-}3\times10^{21}$ cm^{-3}), revealing that the film is highly conductive. This result is consistent with the results obtained in previous work (Ref 17). In the presence of chromate, the donor density drops by one order of magnitude first and then increases gradually, as a result of different susceptibilities to pitting corrosion.

3.6 Electrochemical Impedance Spectroscopy Measurements

Impedance spectra were measured at OCP immersed in solutions for 1.5 h. Figure 10 and 11 show the Nyquist and Bode plots of the samples in various solutions, respectively. This type of diagram is usually interpreted as a mechanism of charge transfer on an inhomogeneous surface (Ref 10, 18). As shown in Fig. 10, the capacitive loops for specimens were broad with adding the concentration of chromate below 0.03 M, indicating better film stability. However, when the chromate above 0.03 M, up to 0.1 M or even higher, the stability of film became weaker.

As shown in Fig. 11, most Bode diagrams consist of two well-defined time constants. The two time constants could be related to two different processes, the first one, obtained in high frequency range, associates with the passive film formed on the sample surface, and the second one, obtained in low frequency range, associates with the charge transfer at substrate/film interface (Ref 18-20).

An electrical equivalent circuit (EEC) showed in Fig. 12 is proposed to interpret the EIS results. This equivalent circuit has been proposed for interpreting the corrosion process of austenitic stainless steels with passive film (Ref 10, 21-23). R_{ct} is charger transfer resistance. CPE_{dl} represents the capacitance of the passive layer including the defects. CPE_{film} is the subsequent passive layer on the metal surface. R_{film} is the passive film resistance, which is used to describe the adsorption of inhibitor. The non-ideal electric behavior is taken into account by introducing a constant phase element (CPE). CPE is defined in impedance representation as:

$$Z(\omega) = Z_0(i\omega)^{-n}, \qquad \text{(Eq 3)}$$

where Z_0 is the CPE constant, ω is the angular frequency, $i^2 = -1$ is the imaginary number, and n is the CPE exponent. The factor n, defined as a CPE power, is an adjustable parameter that always lies between 0.5 and 1. If $n = 1$, the CPE describes an ideal capacitor; for $0.5 < n < 1$, the CPE describes a distribution of dielectric relaxation times in frequency space; when $n = 0.5$, the CPE represents a Warburg impedance with diffusion character. This model assumes that the passive film does not totally cover the metal surface and cannot be considered as a homogeneous layer but rather as a defective layer. In fact, neither real surfaces of solids in the active range nor passive films on metallic substrates can be considered to be ideally homogeneous (Ref 24).

The fitted parameters are listed in Table 3. R_{ct} increased with the increasing of chromate concentration when the chromate concentration is <0.03 M, the R_{ct} reached a maximum value when the chromate concentration is 0.03 M, then the R_{ct} decreased with the increasing of chromate concentration. The value of CPE_{dl} increased with the increasing of the chromate concentration, the increase in CPE_{dl} values was caused by the adsorption of chromate (Ref 7, 10, 25).

4. Discussion

4.1 The Effect of Chromate on the Passive Film

Figure 8 shows the M-S plots of the passive film formed on the 2205 DSS in 1 M NaCl solution. In the zone (I), the positive slope is a characteristic of the n-type semiconductor,

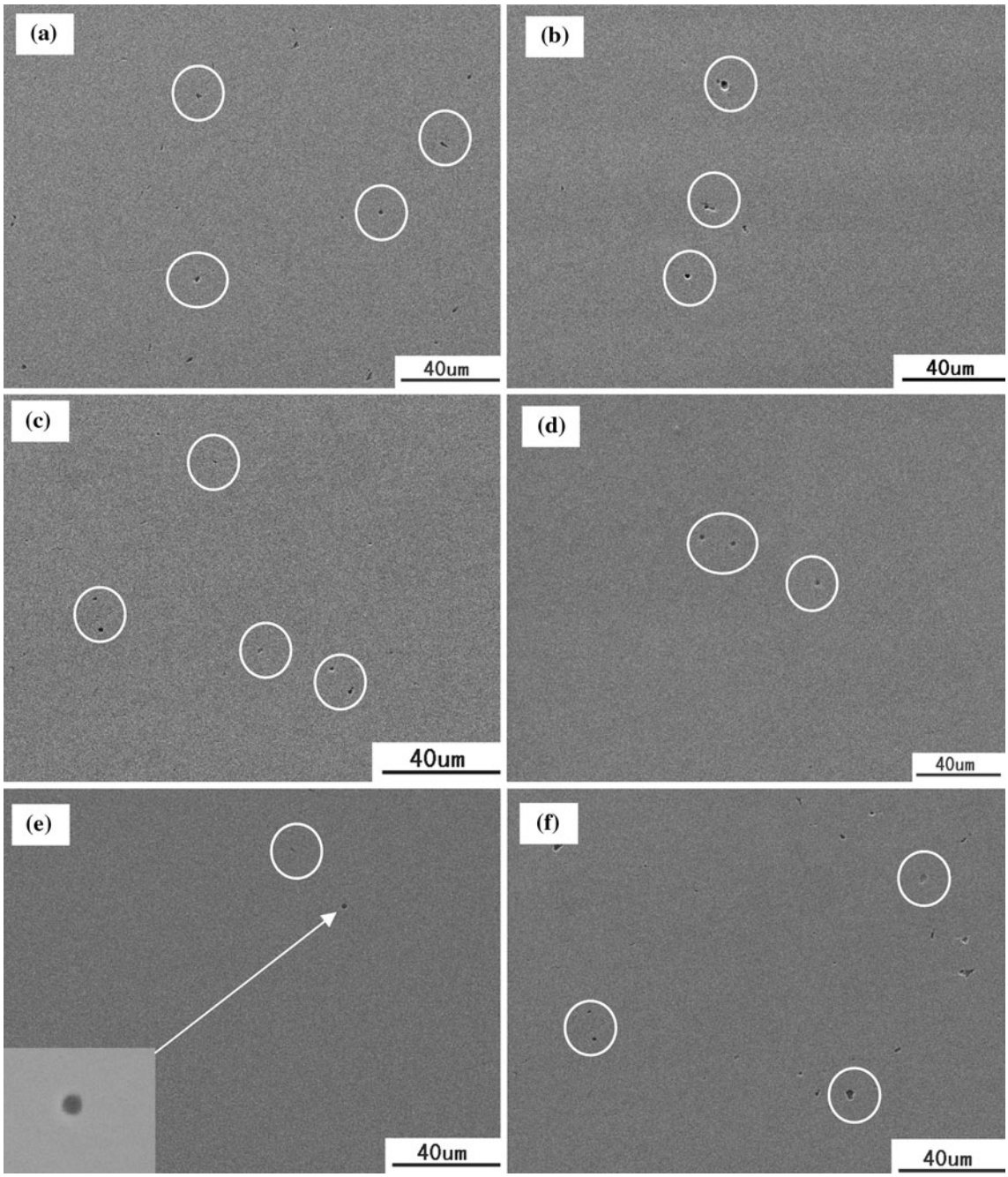

Fig. 7 SEM images of 2205 duplex stainless steel after polarization in NaCl solutions with (a) 0 M CrO_4^{2-}, (b) 0.001 M CrO_4^{2-}, (c) 0.005 M CrO_4^{2-}, (d) 0.01 M CrO_4^{2-}, (e) 0.03 M CrO_4^{2-}, (f) 0.05 M CrO_4^{2-}, (g) 0.1 M CrO_4^{2-}, (h) 0.3 M CrO_4^{2-}, and (I) 0.5 M CrO_4^{2-}

whereas, in the zone (II), the negative slope is the characteristic of the p-type semiconductor (Ref 14).

The M-S plots of the passive films formed on the samples in 1 M NaCl containing different concentration of chromate are shown in Fig. 9. All the M-S plots display three zones: zone (I) and (III) shows one of the characteristics of n-type semiconductors, while zone (II) shows the characteristic of p-type semiconductors. The existence of negative and positive slopes in the curves has been interpreted as the representative of a capacitance behavior. With an inner p-type semiconducting region formed by chromium oxide and an outer n-type semiconducting region formed by iron oxides (Ref 15, 16). At the potential between about 0.3 and 0.85 V, the type of semiconductor changes from p-type response to n-type, indicating the main components of passive film also change from chromium oxides to iron oxides.

From the slope of the straight lines in different zones of $C^{-2} \sim E$ plots, the donor and acceptor densities of the passive film layers developed in NaCl solutions with different concentrations of chromate can be estimated. The data listed in Table 2 shows that the value of the donor and acceptor densities are much higher in NaCl solution without chromate than that in NaCl solution with chromate, the donor density drops by one order of magnitude in the presence of the chromate. In this

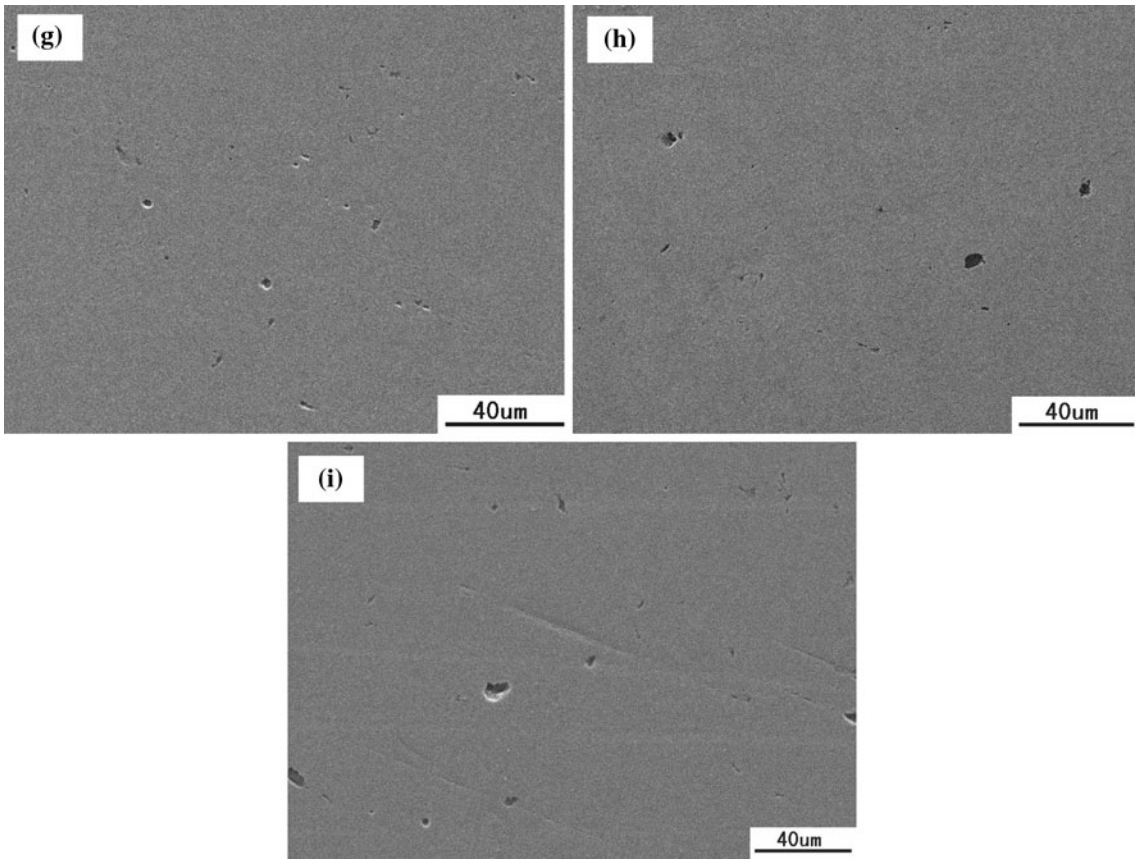

Fig. 7 Continued

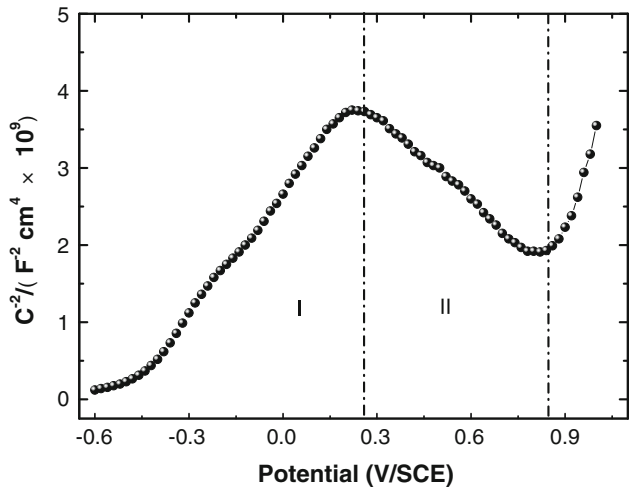

Fig. 8 Mott-Schottky plots of passive film formed on 2205 duplex stainless steel in 1 M NaCl solution without Na_2CrO_4

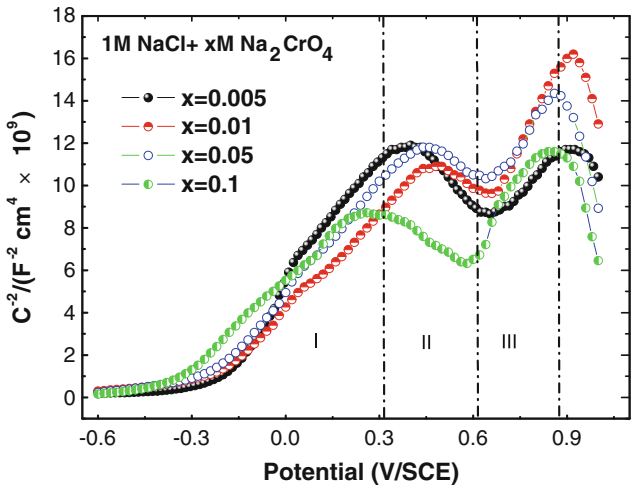

Fig. 9 Mott-Schottky Plots of passive films formed on 2205 duplex stainless steel in 1 M NaCl solutions containing different concentrations of Na_2CrO_4

sense, as the donor or acceptor increased, the chloride ions have higher possibility to attack the passive film, consequently, leading to the occurrence of pitting corrosion.

According to the point defect mode (Ref 26), the chloride ions are transferred from the electrolyte to the oxygen vacancies in the outer passive film, decreasing their concentration and increasing in turn the number of cation vacancies. The chloride ions can be adsorbed from the electrolytic solution into the metallic sites (M) of the oxide, producing cations vacancies (V_M) according to the following reactions (Ref 27):

$$M(\text{film}) + \text{Cl}^-(\text{sol}) \rightarrow M\text{Cl}^-(\text{ads}) + V_M^{2-}(\text{film}) \quad \text{(Eq 4)}$$

$$M\text{Cl}^+(\text{ads}) \rightarrow M^{2+}(\text{sol}) + \text{Cl}^-(\text{sol}) \quad \text{(Eq 5)}$$

Thus, there was more oxygen vacancies in the passive film formed in the NaCl solution. The higher donor concentration of passive film, the more oxygen vacancies there are in the passive film. Oxygen vacancies in the passive film can absorb chloride

Table 2 The donor (N_D) or acceptor (N_A) densities of passive films formed on 2205 duplex stainless steel in 1 M NaCl solutions with different concentrations of Na_2CrO_4

Passive film	Concentration	N_D and N_A (10^{20} at. cm^{-2}) I	II	III
2205	1 M NaCl	16.88	24.63	…
	1 M NaCl + 0.001 M Na_2CrO_4	1.623	2.344	1.274
	1 M NaCl + 0.005 M Na_2CrO_4	4.266	5.473	2.036
	1 M NaCl + 0.01 M Na_2CrO_4	6.028	8.576	4.265
	1 M NaCl + 0.05 M Na_2CrO_4	6.365	8.891	4.289
	1 M NaCl + 0.1 M Na_2CrO_4	6.564	9.881	3.965
	1 M NaCl + 0.5 M Na_2CrO_4	7.381	10.57	4.524

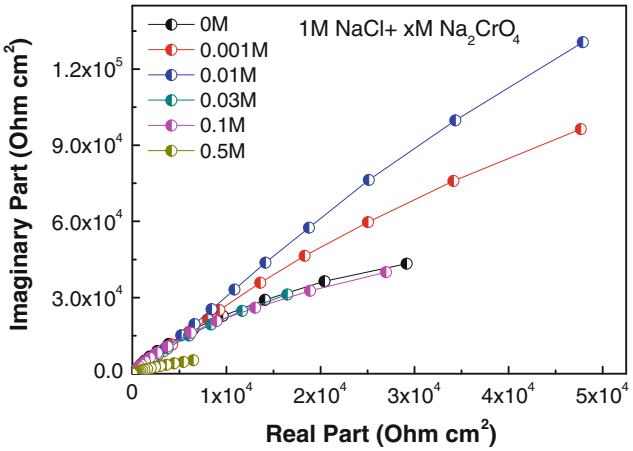

Fig. 10 Nyquist plots of 2205 duplex stainless steel in 1 M NaCl solutions with different concentrations of Na_2CrO_4

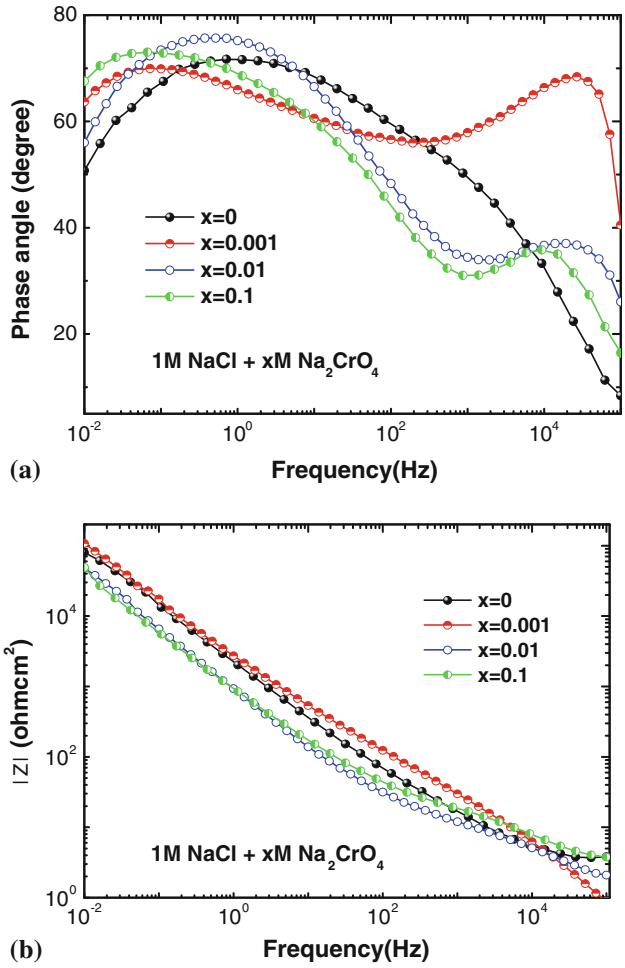

Fig. 11 Bode plots of duplex stainless steel in 1 M NaCl solutions with different concentrations of Na_2CrO_4

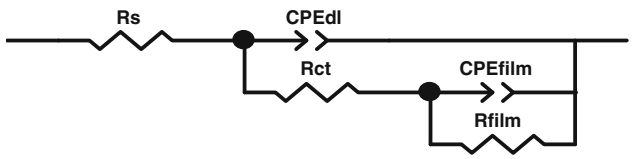

Fig. 12 Electrical equivalent circuit for analysis of EIS results

ions, which leads to the breakdown of the passive film. Therefore, the results obtained from the M-S plots show that the donor density characterizes the affinity of chloride ions for the passive film. These may assume that the sensitivity to pit nucleation increases with the affinity, or occurs when the cation vacancies concentration exceeds a critical value. Therefore, donor density may also feature the pit nucleation ability.

The Bode diagrams of 2205 DSS measured in chromate-containing NaCl solutions are characterized by two times constants due to the addition of chromate resulting in the formation of passive film layer, the same conclusion was obtained by Igual Muñoz et al. (Ref 7). From the fitted EIS results in Table 3, the variation of R_{ct} shows that there is a maximum charge transfer resistance when the chromate concentration is 0.03 M, indicating that the passive film formed in NaCl solution with 0.03 M chromate has the highest corrosion resistance.

The value of CPE_{dl} increases with the increasing of chromate concentration in chromate-containing NaCl solutions. All the CPE_{dl} values measured in chromate-containing NaCl solutions are lower than that in NaCl solution without chromate. In physical terms, CPE_{dl} can either be associated with the capacitance of a compact dielectric oxide film or correspond to the double layer capacitance over the fraction of the area left uncovered by the passivating film (Ref 28). The increase in CPE_{dl} leads to decrease in local dielectric constant or increase in the thickness of the electrical double layer (Ref 7, 8).

Isaacs et al. (Ref 29) proved that Cr(VI) only weakly adsorbed on passive films and could not withstand simple washing of the surface except after exposure to concentrated solutions and only when the growth rate of the oxide has dropped. This means that under these conditions, the Cr(VI) is probably incorporated into the oxide, forming an improved stability against the aggressive ions. In this study, the increase of CPE_{dl} indicates that the exposed area increased may be also due to pitting corrosion. The CPE_{dl} values also correlate with the adsorption of chromate (Ref 30).

The n_{dl} provides a strong capacitive response of the metal/electrolyte interface. If n_{dl} is accepted to be a measure of surface inhomogeneity, then its decrease should be related to certain increase in heterogeneity resulting from metal surface roughening. n_{dl} increases as chromate concentration increased when the chromate concentration is <0.03 M, while n_{dl} decreases with chromate concentration when the chromate

Table 3 EIS fitted parameters of 2205 duplex stainless steel in 1 M NaCl solutions with different concentrations of Na_2CrO_4

Solution	R_s	R_{ct}	CPE_{dl}	n_{dl}	CPE_{film}	n_{film}	R_{film}
1 M NaCl	3.73	435	5.505*E*−05	0.8266	3.966*E*−05	0.8305	4.656*E*+05
1 M NaCl + 0.001 M Na_2CrO_4	1.25	2914	4.407*E*−05	0.8306	3.145*E*−05	0.8803	6.106*E*+05
1 M NaCl + 0.005 M Na_2CrO_4	2.38	3650	4.438*E*−05	0.8516	3.178*E*−05	0.8712	6.089*E*+05
1 M NaCl + 0.01 M Na_2CrO_4	2.48	4700	4.508*E*−05	0.8519	3.365*E*−05	0.8517	5.249*E*+05
1 M NaCl + 0.03 M Na_2CrO_4	2.50	4730	4.528*E*−05	0.8520	3.505*E*−05	0.8402	4.895*E*+05
1 M NaCl + 0.05 M Na_2CrO_4	2.45	4706	5.579*E*−05	0.8029	4.307*E*−05	0.8289	4.006*E*+05
1 M NaCl + 0.1 M Na_2CrO_4	3.81	4700	5.654*E*−05	0.7935	4.826*E*−05	0.8274	3.599*E*+05
1 M NaCl + 0.3 M Na_2CrO_4	4.35	4225	5.642*E*−05	0.7891	4.834*E*−05	0.8101	3.344*E*+05
1 M NaCl + 0.5 M Na_2CrO_4	4.92	3833	5.742*E*−05	0.7591	4.898*E*−05	0.7889	3.054*E*+05

concentration is >0.03 M, indicating that the capacitive interface is weakened, because the passive layer became more conductive with the increasing number of opening pits (Ref 7, 10).

The relationship between C, dielectric constant and the thickness of the passive films is as follows (Ref 23):

$$C = \frac{(QR)^{1/n}}{R} \quad \text{(Eq 6)}$$

$$d = \frac{\varepsilon\varepsilon_0 A}{C} \quad \text{(Eq 7)}$$

where ε_0 is the permittivity of vacuum, ε is the dielectric constant, A is the effective area, Q is the CPE values, and d is the thickness of electrical double layer. It is difficult to obtain an accurate thickness, but the passive film thickness is proportional to $1/CPE_{film}$. Hence, the capacitive responses in solution with different concentrations of chromate can provide an indication of the thickness of passive film. The passive film thickness increased with the increasing of chromate concentration. On the contrary, the passive film thickness decreased with the increasing of chromate concentration when the chromate concentration is >0.03 M, which may be due to the fact that the capacitive interface was weakened and the increasing number of opening pinholes (Ref 20). The decrease of R_{film} on one hand may be attributed to the corrosion rate increase, and on the other hand to the probable desorption of the inhibitor (Ref 10, 31). The EIS results are in agreement with the M-S and polarization curves results. Furthermore, the SEM results also proved that the best passive film with only few metastable pits was obtained in NaCl solution with 0.03 M chromate.

4.2 The Effect of Chromate on the Pitting

2205 DSS was spontaneously passivated in NaCl media, which is in accordance with its high corrosion resistance. The passivity properties were enhanced by the chromate, which can be proved quantitatively by the i_p. The i_p of 2205 DSS in 1 M NaCl solution without chromate is about 0.8 μA/cm^2, and then became much lower by adding different concentrations of chromate. The inhibiting effect of chromate can be explained on the basis of the competitive adsorption between the inorganic anions and the aggressive Cl^- ions on the passive electrode surface. According to the possible reactions, chromate reduction products are expected to deposit on the metal surface, especially at the sites of inclusions, which are supposed to be more active than the rest of the surface.

As the potential reaches E_p, the i_p rises steeply without any sign of oxygen evolution. The breakdown of the passive film and the initiation of pitting attack could be due to the ability of Cl^- ions to penetrate the passive film. With the assistance of a high electric field, Cl^- ions can across the passive film and attack the surface of metal substrate. Or the Cl^- ions would displace the adsorbed passivating species at some locations as a result of accelerating local anodic dissolution (Ref 10).

With the addition of chromate <0.03 M, the increasing of chromate concentration leads the E_p shifted toward the positive direction. This suggests that the chromate blocks the reactive sites on the surface of 2205 DSS. The inhibition behavior of chromate may be explained by the difference between the polarizability of chromate and chloride ions (Ref 6, 32). The CrO_4^{2-} anions have higher specific adsorption than the Cl^- ions, which means that CrO_4^{2-} anions can displace the adsorbed Cl^- ions to increase the protectiveness of the passive film. Refaey (Ref 33) also obtained the similar conclusion in chloride-containing solutions. However, when the chromate concentration is >0.03 M, E_p shifted to negative direction and i_p began to increase. The increasing of chromate concentration leads the E_p shifted toward the negative direction, which means that the DSS becomes more susceptible to pitting corrosion. The chromate inhibiting effect decreases due to it acts as a cathodic polarizer when the chromate in high concentration (Ref 34). The SEM images provide direct evidence to prove the electrochemical results, it has been established that chromate affected pit nucleation by reducing the total number, and size of corrosion pit.

5. Conclusions

The 2205 DSS can be passivated in 1 M NaCl solution no matter with or without chromate. The addition of chromate is able to enhance the passivity of the 2205 DSS. The electrochemical behavior of 2205 DSS is heavily dependent on the chromate concentration.

The presence of chromate improves the stability of passive film; the most stable passive film was formed in 1 M NaCl solution with 0.03 M chromate. The addition of chromate changes semiconducting properties of the passive film. The passive film formed in NaCl solution without chromate only has two zones, while the passive film formed in NaCl solution with chromate is characterized by three zones. The semiconducting property of the passive film is potential-dependent, Fe-rich n-type oxide and Cr-rich p-type oxide dominated at different potential ranges.

There was a critical chromate concentration value of 0.03 M in the 1 M NaCl solutions, below which the pitting susceptibility on the stainless steel would be inhibited and above which it would be accelerated. Moreover, the variation of chromate concentration changes pit number, pit size, as well as the frequency of occurrence of pit.

Acknowledgments

This study was financially supported by Chinese National Science and Technology Infrastructure Platforms Construction Project (No. 2005DKA10400).

References

1. H. Eriksson and S. Bernhardsson, The Applicability of Duplex Stainless Steels in Sour Environments, *Corrosion*, 1991, **47**, p 719–727
2. V. Muthupandi, P. Bala Srinivasan, and S.K. Seshadri, Effect of Weld Metal Chemistry and Heat Input on the Structure and Properties of Duplex Stainless Steel Weld, *Mater. Sci. Eng. A*, 2003, **358**, p 9–16
3. A. Kocijan, D. Kek-Merl, and M. Jenko, The Corrosion Behaviour of Austenitic and Duplex Stainless Steels in Artificial Saliva with the Addition of Fluoride, *Corros. Sci.*, 2011, **53**, p 776–783
4. C.-O.A. Olsson and D. Landolt, Passive Films on Stainless Steels-Chemistry, Structure and Growth, *Electrochim. Acta*, 2003, **48**, p 1093–1104
5. P. Ernst and R.C. Newman, Pit Growth Studies in Stainless Steel Foils—I, Introduction and Growth Kinetics, *Corros. Sci.*, 2002, **44**, p 927–941
6. S.A.M. Refaey, S.S. Abd El-Rehim, F. Taha et al., Inhibition of Chloride Localized Corrosion of Mild Steel by PO_4^{3-}, CrO_4^{2-}, MoO_4^{2-} and NO_2^- anions, *Appl. Surf. Sci.*, 2000, **158**, p 190–196
7. A. Igual Muñoz, J. García Antón, J.L. Guiñón et al., The Effect of Chromate in the Corrosion Behaviour of Duplex Stainless Steel in LiBr Solutions, *Corros. Sci.*, 2006, **48**, p 4127–4151
8. A. Igual Muñoz, J. García Antón, J.L. Guiñón et al., Comparison of Inorganic Inhibitors of Copper, Nickel and Copper-Nickels in Aqueous Lithium Bromide Solution, *Electrochim. Acta*, 2004, **50**, p 957–966
9. Y.F. Cheng and J.L. Luo, Passivity and Pitting of Carbon Steel in Chromate Solutions, *Electrochim. Acta*, 1999, **44**, p 4795–5804
10. A. Igual Muñoz, J. García Antón, J.L. Guiñón et al., Inhibition Effect of Chromate on the Passivation and Pitting Corrosion of a Duplex Stainless Steel in LiBr Solutions Using Electrochemical Techniques, *Corros. Sci.*, 2007, **49**, p 3200–3225
11. M.H. Dean and U. Stimming, The Electronic Properties of Disordered Passive Films, *Corros. Sci.*, 1989, **29**, p 199–211
12. G.O. Ilevbare and G.T. Burstein, The Inhibition of Pitting Corrosion of Stainless Steels by Chromate and Molybdate Ions, *Corros. Sci.*, 2003, **45**, p 1545–1569
13. M.J. Carmezim, A.M. Simões, M.F. Montemor et al., Capacitance Behavior of Passive Films on Ferritic and Austenitic Stainless Steel, *Corros. Sci.*, 2005, **47**, p 581–591
14. M.F. Montemor, M.G.S. Ferreira, N.E. Hakiki et al., Chemical Composition and Electronic Structure of the Oxide Films Formed on 316L Stainless Steel and Nickel Based Alloys in High Temperature Aqueous Environments, *Corros. Sci.*, 2000, **42**, p 1635–1650
15. N.E. Hakiki, M.F. Montemor, M.G.S. Ferreira et al., Semiconducting Properties of Thermally Grown Oxide Films on AISI, 304 Stainless Steel, *Corros. Sci.*, 2000, **42**, p 687–702
16. D. Shintani, T. Ishida, H. Izumi et al., XPS Studies on Passive Film Formed on Stainless Steel in a High-Temperature and High-Pressure Methanol Solution Containing Chloride Ions, *Corros. Sci.*, 2008, **50**, p 2840–2845
17. M.Z. Yang, J.L. Luo, and B.M. Patchet, Correlation of Hydrogen-Facilitated Pitting of AISI, 304 Stainless Steel to Semiconductivity of Passive Films, *Thin Solid Films*, 1999, **354**, p 142–147
18. A.C. Bastos, M.G.S. Ferreira, and A.M. Simoes, Comparative Electrochemical Studies of Zinc Chromate and Zinc Phosphate as Corrosion Inhibitors for Zinc, *Prog. Inorg. Coat.*, 2005, **52**, p 339–350
19. C. Liu, Q. Bi, A. Leyland, and A. Matthews, An Electrochemical Impedance Spectroscopy Study of the Corrosion Behaviour of PVD Coated Steels in 0.5 N NaCl Aqueous Solution: Part I. Establishment of Equivalent Circuits for EIS Data Modeling, *Corros. Sci.*, 2003, **45**, p 1243–1256
20. C. Liu, Q. Bi, and A. Matthews, EIS Comparison on the Corrasion Performance of PVD TiN and CrN Coated Mild Steel in 0.5 N NaCl Aqueous Solution, *Corros. Sci.*, 2001, **43**, p 1953–1961
21. J.H. Lee, S.H. Ahn, and J.G. Kim, Effect of Al Additions in WC-(Cr1-xAlx)N Coatings on the Corrosion Resistance of Coated AISI, D2 Steel in a Deaerated 3.5 wt% NaCl Solution, *Surf. Coat. Technol.*, 2005, **190**, p 417–425
22. C.M. Abreu, M.J. Cristóbal, R. Losada et al., High Frequency Impedance Spectroscopy Study of Passive Films Formed on AISI, 316 Stainless Steel in Alkaline Medium, *J. Electroanal. Chem.*, 2004, **572**, p 335–345
23. C.T. Liu and J.K. Wu, Influence of pH on the Passivation Behavior of 254SMO Stainless Steel in 3.5% NaCl Solution, *Corros. Sci.*, 2007, **49**, p 2198–2209
24. P. Girault, J.L. Grosseau-Poussard, J.F. Dinhut et al., Influence of a Chromium Ion Implantation on the Passive Behaviour of Nickel in Artificial Sea-Water: An EIS and XPS Study, *Nucl. Instrum. Methods Phys. Res. B*, 2001, **174**, p 439
25. A. Igual Muñoz, J. García Antón, J.L. Guiñón et al., Corrosion Studies of Austenitic and Duplex Stainless Steels in Aqueous Lithium Bromide Solution at Different Temperatures, *Corros. Sci.*, 2004, **46**, p 2955–2974
26. D.D. McDonald, The Point Defect Model for the Passive State, *J. Electrochem. Soc.*, 1992, **139**, p 3434–3449
27. J. Amri, T. Souier, B. Malki, and B. Baroux, Effect of the Final Annealing of Cold Rolled Stainless Steels Sheets on the Electronic Properties and Pit Nucleation Resistance of Passive Films, *Corros. Sci.*, 2008, **50**, p 431–438
28. R.L. Zeller, III, and R.F. Savinell, Computational Analysis Methods to Quantify a.c. Impedance Data, *Corros. Sci.*, 1986, **26**, p 591–599
29. H.S. Isaacs, S. Virtanen, M.P. Ryan et al., Incorporation of Cr in the Passive Film on Fe from Chromate Solutions, *Electrochim. Acta*, 2002, **47**, p 3127–3130
30. S. Tamil Sevil, V. Raman, and N. Rajendran, Corrosion Inhibition of Mild Steel by Benzotriazole Derivatives in Acidic Medium, *J. Appl. Electrochem.*, 2003, **33**, p 1175–1182
31. C. Fonseca and M. Barbosa, Corrosion Behaviour of Titanium in Biofluids Containing H_2O_2 Studied by Electrochemical Impedance Spectroscopy, *Corros. Sci.*, 2001, **43**, p 547–559
32. S.A.M. Refaey and S.S. Abd El Rehim, Inhibition of Chloride Pitting Corrosion of Tin in Alkaline and Near Neutral Medium by Some Inorganic Anions, *Electrochim. Acta*, 1997, **42**, p 661–674
33. S.A.M. Refaey, Inhibition of Steel Pitting Corrosion in HCl by Some Inorganic Anions, *Appl. Surf. Sci.*, 2005, **240**, p 396–404
34. A. Bahadur, Development and Evaluation of a Low Chromate Corrosion Inhibitor for Cooling Water Systems, *Can. Metall. Q.*, 1998, **37**, p 459–468